Chapter

Integral Backstepping Controller for UAVs Team Formation

Wesam M. Jasim and Dongbing Gu

Abstract

In this chapter, two controllers are investigated for stabilisation, path tracking and leader-follower team formation. The first controller is a PD2 implemented for attitude stability. The second controller is an Integral Backstepping IBS control algorithm presented for the path tracking and leader-follower team formation problems of quadrotors. This nonlinear control technique divide the control into two loops, the inner loop is for the attitude stabilisation and the outer loop is for the position control. The dynamic model of a quadrotor is represented based on Euler angles representation and includes some modelled aerodynamical effects as a nonlinear part. The IBS controller is designed for the translational part to track the desired trajectory and to track the leader quadrotor by the followers. Stability analysis is achieved via a suitable Lyapunov function. The external disturbance and model parameters uncertainty are considered in the simulation tests. The proposed controllers yielded good results in terms of Root Mean Square Error RMSE values, time-consumption, disturbance rejection and model parameter uncertainties change coverage.

Keywords: integral backstepping, adaptive controller, Euler angles, UAVs quadrotors, team formation

1. Introduction

In recent years, research on the control of Unmanned Aerial Vehicles (UAVs) has been growing due to its simplicity in design and low cost. Quadrotor helicopters have several advantages over fixed-wing air crafts, such as taking off and landing vertically in a limited space and hovering easily over fixed or dynamic targets, which gives them efficiency in applications that fixed-wing air crafts cannot do, in addition to being safer [1–3]. Based on its structure the UAV offers the power of sensing and computing in many applications. Quadrotor UAVs can be used to perform several tasks in the applications of dangerous areas for a manned aircraft in a high level of accuracy. They can be utilised in different applications, such as inspection of power lines, oil platforms, search and rescue operations, and surveillance [4–6]. Increasing the applications of quadrotors encourages the growth in their technologies and raises the requirements on autonomous control protocols. Moreover, using swarm robotics has advantages over individual robots in that they perform their tasks faster with high accuracy and use a minimum number of sensors by distributing them to the robots [7]. Researchers are focusing on the design and implementation of many types of controllers to control the take-off, landing and

hovering of individual quadrotor UAVs with some applications which require the creation of a trajectory and tracking in three dimensions, benefiting from the wide developments in sensors.

Research in the field of control of individual and multi-robot quadrotor team formation is still facing some challenges. Challenges of individual quadrotor control come from the complexity of modelling its dynamic system because of its complex structure and the design issue. The dynamic model equations present four input forces with six output states, which mean that the system is in under-actuated range [5, 7]. Further challenges of multi-robot control come from evaluating the control architecture and communication network limitations.

The formation problem of quadrotors has had a vast area of interesting research in the past few years. Researchers have been motivated to contribute to this field of research by the development of materials, sensors and electronics used in designing quadrotors, which consequently has an effect on minimising their size, weight and cost. Working as a team of quadrotors has many benefits over using a single quadrotor in several applications.

Team formation control includes many problems to be addressed, including communication loss, delay between the robots or packet drop problems [8–11]. Simultaneous localization and mapping is another problem in team formation control, in which the vehicle builds up its maps and estimates its location precisely at the same time; this problem has also been addressed in [12–14]. The third problem is the collision and obstacle avoidance, which includes avoiding collisions with both other robots and static or moving unknown obstacles while flying to their destination and maintaining their positions. Solutions to this problem have been handled by [12, 15]. Now, team formation control adopts a combination of some functions; the first is to perform the mission between two points, the second is to preserve the comparative positions of the robots over the formation and maintain the shape consequently, the third is to avoid obstacles and the forth is to divide the formation. In this chapter, we focus on designing only a control law for the leader-follower team formation problem with collision avoidance between team members by maintaining the distance between the leader and the follower.

In the leader-follower approach, at least one vehicle performs as a leader and the other robots are followers. The leader vehicle tracks a predefined path, whereas the followers maintain a certain distance with the leader and among themselves to obtain the desired shape. Each robot has its own controller and the robots keep the desired relative distance between themselves. However, two types of control architecture may be used to control the vehicle: one loop control scheme and two loop control scheme. If a two loop control scheme is used to control each vehicle, the outer loop is used for position control and its x and y output is the desired roll and pitch angles. These desired angles with the desired yaw angle are used to calculate the vehicle torques; in other words, they stabilise the quadrotor angles. This type of control is built according to time scale separation, where the attitude dynamics are much faster than translation dynamics. In the one loop control scheme, on the other hand, separation of the vehicle dynamics to attitude and translation is not considered. In this case, the position tracking error is used directly to calculate the vehicle torques to achieve its path tracking. According to these definitions, leader-follower team formation requires attitude stabilisation and path tracking to be achieved.

Abundant literature exists on the subject of attitude stabilisation, path tracking and leader-follower team formation control. Several control techniques have been demonstrated to control a group of quadrotors varying between the linear PID, PD or LQR controllers to more complex nonlinear controllers as neural networks and BS controllers. These controllers achieved good results and some of them

guaranteed the performance, such as the LQR controller, and some of them guaranteed their stability. The performance of an individual quadrotor or a group of quadrotors in formation control is often affected by external disturbances such as payload changes (or mass changes), wind disturbance, inaccurate model parameters, etc. Therefore, the IBS controller was proposed to reject the effect of disturbances and handle the change in model parameter uncertainties. On the other hand, improving the control performance is another aspect.

Dynamic model representation of the quadrotors is a major demand for designing these controllers. In this chapter, Euler angles technique was used to represent the quadrotors.

2. Dynamic model

In this section, Euler angles are used to represent the quadrotor dynamical model. External disturbances and model parameter uncertainties change are considered as well. An IBS controller is derived and tested in simulation. The stability analysis is obtained via a selected Lyapunov function. The full quadrotor dynamic model including the gyroscope effects $G(\omega)$ is

$$\begin{cases} \dot{\mathbf{p}} = \mathbf{v} \\ \dot{\mathbf{v}} = -g\mathbf{e} + \dfrac{f}{m} R_\theta \mathbf{e} \\ \dot{R}_\theta = R_\theta S(\omega) \\ J\dot{\omega} = -S(\omega)J\omega - G(\omega) + \tau_E \end{cases} \tag{1}$$

and the rotational matrix R_θ from the inertial frame to the body frame is

$$R_\theta = \begin{bmatrix} c\psi c\theta & c\psi s\theta s\varphi - s\psi c\varphi & c\psi s\theta c\varphi + s\psi s\varphi \\ s\psi c\theta & s\psi s\theta s\varphi + c\psi c\varphi & s\psi s\theta c\varphi - c\psi s\varphi \\ -s\theta & c\theta s\varphi & c\theta c\varphi \end{bmatrix}. \tag{2}$$

where m is the quadrotor mass, $\omega = \left[\omega_x, \omega_y, \omega_z\right]^T$ is the angular velocity in the body frame, J is the 3×3 diagonal matrix representing three inertial moments in the body frame, τ_E is the torque vector applied on the quadrotor, $\mathbf{v} = \left[v_x, v_y, v_z\right]^T$ is the linear velocity, $\mathbf{p} = [x, y, z]^T$ is the position vector, S is the skew-symmetric cross product matrix, and the vector $\mathbf{e} = [0, 0, 1]^T$.

Assuming that φ, θ, ω_x, ω_y and ω_z are very small, $\zeta = [\varphi, \theta, \psi]^T$, $\eta = \dot{\zeta} = \left[\dot{\varphi}, \dot{\theta}, \dot{\psi}\right]^T = \left[\omega_x, \omega_y, \omega_z\right]^T$ and $\dot{\eta} = \left[\ddot{\varphi}, \ddot{\theta}, \ddot{\psi}\right]^T = \left[\dot{\omega}_x, \dot{\omega}_y, \dot{\omega}_z\right]^T$, then the attitude control part of Eq. (1) can be written as:

$$\begin{cases} f = mg \\ \ddot{\varphi} = \dot{\theta}\dot{\psi}\dfrac{J_y - J_z}{J_x} + \dfrac{J_r}{J_x}\dot{\theta}\Omega + \dfrac{\tau_\varphi}{J_x} \\ \ddot{\theta} = \dot{\varphi}\dot{\psi}\dfrac{J_z - J_x}{J_y} - \dfrac{J_r}{J_y}\dot{\varphi}\Omega + \dfrac{\tau_\theta}{J_y} \\ \ddot{\psi} = \dot{\varphi}\dot{\theta}\dfrac{J_x - J_y}{J_z} + \dfrac{\tau_\psi}{J_z} \end{cases} \tag{3}$$

3. Quadrotors formation problem

The full dynamic model based on Euler angles (1) of a quadrotor can be written as:

$$\begin{cases} \dot{\mathbf{p}}_i = \mathbf{v}_i \\ \dot{\mathbf{v}}_i = -g\mathbf{e} + \dfrac{f_i}{m_i} R_{i\theta}\mathbf{e} \\ \dot{\zeta}_i = \eta_i \\ J_i\dot{\eta}_i = S(\eta_i)J_i\eta_i + G(\eta_i) - \tau_{iE} \end{cases} \tag{4}$$

where i is L for the leader and F for the follower.

The leader-follower formation control problem to be solved in this chapter is a distributed control scheme of one leader and one follower. The leader control problem is formulated as a trajectory tracking, and the follower control problem is also formulated as a tracking problem, but with a different tracking target.

The follower keeps its yaw angle the same as the leader when it maintains the formation pattern. It moves to a desired position $\mathbf{p}_{Fd}$, which is determined by a desired distance d, a desired incidence angle ρ, and a desired bearing angle σ. A new frame F' is defined by the translation of the leader frame L to the frame with the desired follower position $\mathbf{p}_{Fd}$ as the origin. As shown in **Figure 1**, the desired incidence angle is measured between the desired distance d and the $x-y$ plane in the new frame F', and the desired bearing angle is measured between the x axis and the projection of the d in $x-y$ plane in the new frame F'. The desired position $\mathbf{p}_{Fd}$ is

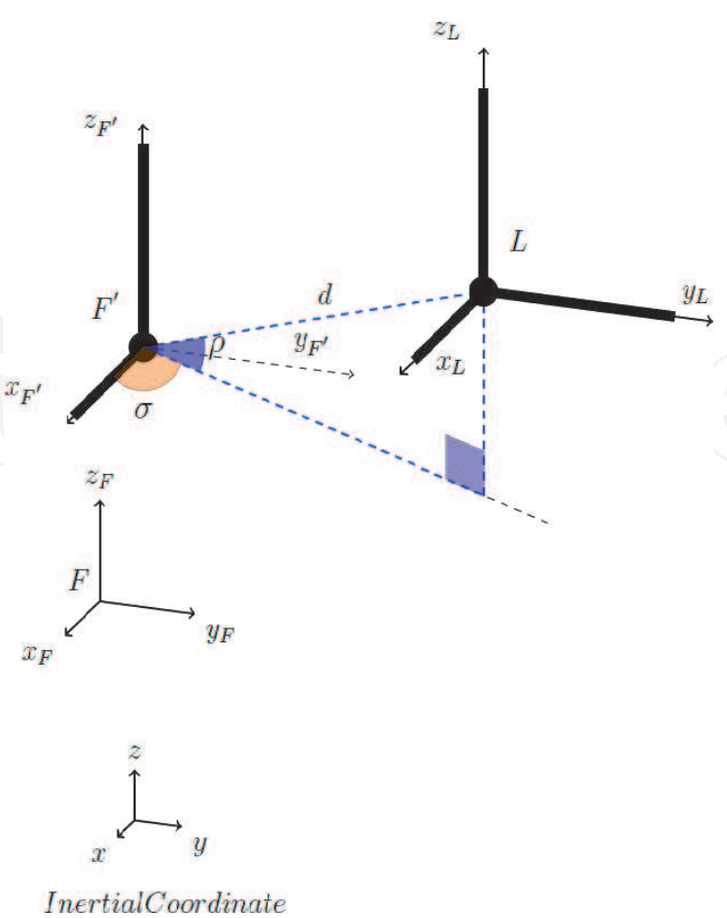

Figure 1.
Body frames in formation.

$$\mathbf{p}_{Fd} = \mathbf{p}_L - R_{Lq}^T d \begin{bmatrix} \cos\rho\cos\sigma \\ \cos\rho\sin\sigma \\ \sin\rho \end{bmatrix}. \tag{5}$$

Assume both the leader and the follower are able to obtain their own pose information and the follower is able to obtain the leader's pose information via wireless communication. The design goal of the controllers is to find the state feedback control law for the thrust and torque inputs for both the leader and the follower. The leader-follower formation control problem is solved if both conditions (6) and (7) are satisfied.

$$\begin{cases} \lim_{t\to\infty}(\mathbf{p}_{Fd} - \mathbf{p}_F) = 0 \\ \lim_{t\to\infty}(\psi_L - \psi_F) = 0 \end{cases} \tag{6}$$

and

$$\begin{cases} \lim_{t\to\infty}(\mathbf{p}_{Ld} - \mathbf{p}_L) = 0 \\ \lim_{t\to\infty}(\psi_{Ld} - \psi_L) = 0 \end{cases} \tag{7}$$

The communication among the robots is assumed to be available. The position $\mathbf{p}_L$, yaw angle ψ_L of the leader L and its first and second derivatives $\dot{\psi}_L$ and $\ddot{\psi}_L$ are assumed to be available and measurable. The linear velocity of the leader L and its derivatives $\mathbf{v}_L$ and $\dot{\mathbf{v}}_L$ are assumed bounded and available for the follower.

4. Formation IBS controllers

Integral backstepping control is one of the popular control approaches for both individual and multiple quadrotors. In this section, the integral backstepping control is applied for the individual quadrotor path tracking and leader-follower formation problems. This nonlinear control technique divide the control into two loops, the inner loop is for the attitude stabilisation and the outer loop is for the position control as shown in **Figure 2**.

In this case, the leader and the follower desired roll and pitch angles are assumed to be $\theta_{Ld} = \theta_{Fd} = 0$ and $\varphi_{Ld} = \varphi_{Fd}$. The dynamic model of a quadrotor is

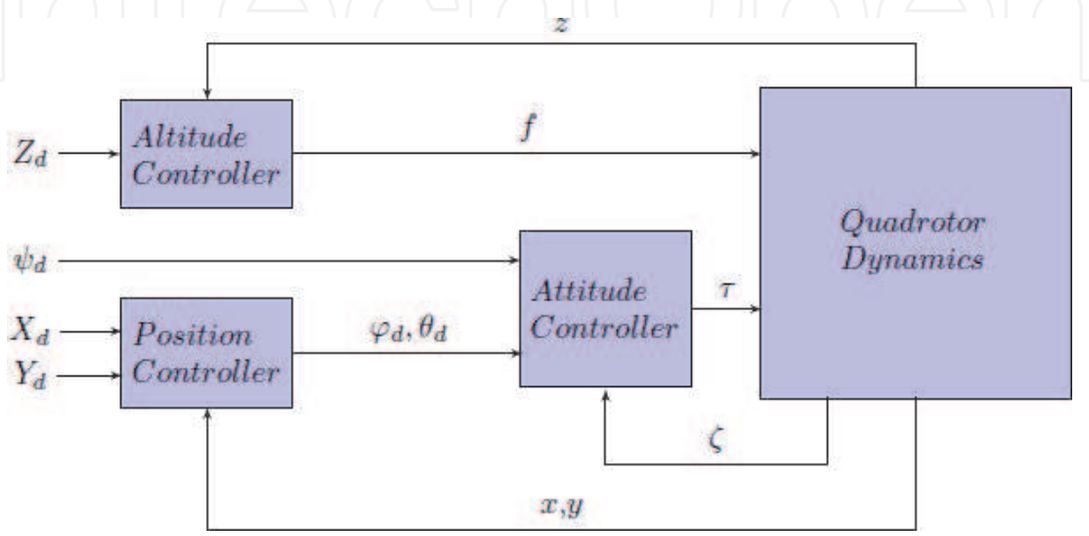

Figure 2.
Two-loop control block diagram.

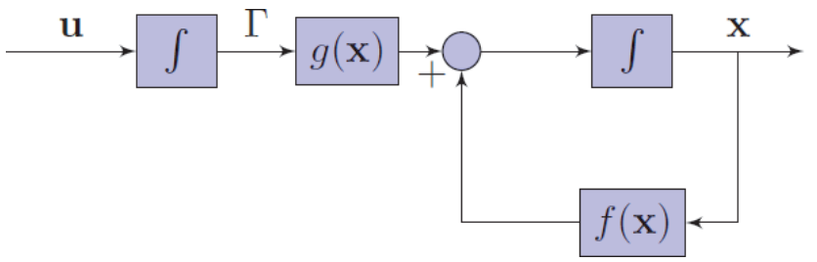

Figure 3.
Initial system.

represented based on Euler angles representation and includes some modelled aerodynamical effects as a nonlinear part. The IBS controller is designed for the translational part to track the desired trajectory. Stability analysis is achieved via a suitable Lyapunov function. The external disturbance and model parameters uncertainty are considered in the simulation tests in all circumstances.

4.1 Backstepping control concept

Backstepping is a recursive design mechanism to asymptotically stabilise a controller for the following system [16]:

$$\begin{cases} \dot{\mathbf{x}} = f(\mathbf{x}) + g(\mathbf{x})\Gamma \\ \dot{\Gamma} = \mathbf{u} \end{cases}. \tag{8}$$

This system is described as an initial system in **Figure 3**, where $\mathbf{x} \in \mathbb{R}^n$ and $\Gamma \in \mathbb{R}$ are the system state and $\mathbf{u} \in \mathbb{R}$ is the control input. $f, g : \mathcal{D} \to \mathbb{R}^n$ are assumed to be smooth and $f(0) = 0$. A stabilising state feedback control law $\Gamma = \Phi(\mathbf{x})$, assuming $\Phi(0) = 0$, exists, in addition to a Lyapunov function $V_1 : \mathcal{D} \to \mathbb{R}^+$ such that

$$\dot{V}_1(\mathbf{x}) = \frac{\partial V_1}{\partial \mathbf{x}}[f(\mathbf{x}) + g(\mathbf{x})\Phi(\mathbf{x})] \leq -V_\varepsilon(\mathbf{x}), \forall \mathbf{x} \in \mathcal{D} \tag{9}$$

where $V_\varepsilon(\mathbf{x}) : \mathcal{D} \to \mathbb{R}^+$ is a positive semidefinite function. Now, the following algebraic manipulation is required: by adding and subtracting the term $g(\mathbf{x})\Phi(\mathbf{x})$ to/from the subsystem (8) we can have the following system:

$$\dot{\mathbf{x}} = f(\mathbf{x}) + g(\mathbf{x})\Phi(\mathbf{x}) + g(\mathbf{x})s \tag{10}$$

where $s = \Gamma - \Phi(\mathbf{x})$, by this construction, when $s \to 0$, $\dot{\mathbf{x}} = f(\mathbf{x}) + g(\mathbf{x})\Phi(\mathbf{x})$ which is asymptotically stable. The derivative of s is

$$\dot{s} = \dot{\Gamma} - \dot{\Phi}(\mathbf{x}) = \mathbf{u} - \dot{\Phi}(\mathbf{x}) = \upsilon \tag{11}$$

which is the backstepping, since $\Phi(\mathbf{x})$ is stepped back by differentiation as described in **Figure 4**. So we have

$$\begin{aligned} \dot{\mathbf{x}} &= f(\mathbf{x}) + g(\mathbf{x})\Phi(\mathbf{x}) + g(\mathbf{x})s \\ \dot{s} &= \upsilon \end{aligned} \tag{12}$$

This system is equivalent to the initial system (8), where $\dot{\Phi} = \frac{\partial \Phi}{\partial \mathbf{x}}\dot{\mathbf{x}} = \frac{\partial \Phi}{\partial \mathbf{x}}[f(\mathbf{x}) + g(\mathbf{x})\Gamma]$. The next step is to stabilise the system (12), and the following Lyapunov function is considered:

$$V(\mathbf{x}, s) = V_1(\mathbf{x}) + \frac{1}{2}s^2. \tag{13}$$

Then

$$\begin{aligned} \dot{V} &= \frac{\partial V_1}{\partial \mathbf{x}}[f(\mathbf{x}) + g(\mathbf{x})\Phi(\mathbf{x}) + g(\mathbf{x})s] + sv \\ &\leq -V_\varepsilon(\mathbf{x}) + \left[\frac{\partial V_1}{\partial \mathbf{x}}g(\mathbf{x}) + v\right]s. \end{aligned} \tag{14}$$

Let

$$\begin{cases} v = -\dfrac{\partial V_1}{\partial \mathbf{x}}g(\mathbf{x}) - \varepsilon s \\ \varepsilon > 0 \end{cases}. \tag{15}$$

Then

$$\dot{V} \leq -V_\varepsilon(\mathbf{x}) - \varepsilon s^2 < 0. \tag{16}$$

This signifies that the origin $(\mathbf{x} = 0, s = 0)$ is asymptotically stable. Since , then the origin $\mathbf{x} = 0$ and $\Gamma = 0$ is also asymptotically stable. In the next step an integral part is added to the BS controller to eliminate the steady state error which occurred in the simulation results and is called IBS.

4.2 Follower integral backstepping controller

The IBS controller for the follower is to track the leader and maintain a desired distance between them with desired incidence and bearing angles.

In this subsection, we derive the IBS controller for the follower. Let us use the follower translational part (17):

$$\ddot{\mathbf{p}}_F = f(\mathbf{p}_F) + g(\mathbf{p}_F)f_F \tag{17}$$

where

$$f(\mathbf{p}_F) = [0 \;\; 0 \;\; -g]^T \tag{18}$$

$$g(\mathbf{p}_F) = \left[u_{Fx}/m_F \quad u_{Fy}/m_F \quad c\theta_F c\varphi_F/m_F\right]^T \tag{19}$$

where

$$u_{Fx} = (c\psi_F s\theta_F c\varphi_F + s\psi_F s\varphi_F) \tag{20}$$

$$u_{Fy} = (s\psi_F s\theta_F c\varphi_F - c\psi_F s\varphi_F). \tag{21}$$

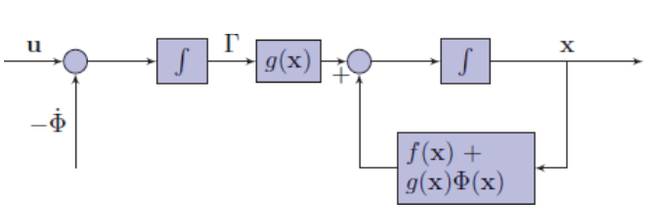

Figure 4.
Backstepping system.

Then the position tracking error between the leader and the follower can be calculated as:

$$\tilde{\mathbf{p}}_F = \mathbf{p}_{Fd} - \mathbf{p}_F = \mathbf{p}_L - R_L^T d \begin{bmatrix} \cos\rho\cos\sigma \\ \cos\rho\sin\sigma \\ \sin\rho \end{bmatrix} - \mathbf{p}_F \tag{22}$$

and its derivative is

$$\dot{\tilde{\mathbf{p}}}_F = \dot{\mathbf{p}}_{Fd} - \dot{\mathbf{p}}_F = \dot{\mathbf{p}}_{Fd} - \mathbf{v}_F \tag{23}$$

where $\mathbf{v}_F$ is a virtual control, and its desirable value can be described as:

$$\mathbf{v}_F^d = \dot{\mathbf{p}}_{Fd} + b_F\tilde{\mathbf{p}}_F + k_F\overline{\mathbf{p}}_F \tag{24}$$

where the integration of the follower position error is added to minimise the steady-state error.

Now, consider the linear velocity error between the leader and the follower as:

$$\tilde{\mathbf{v}}_F = \mathbf{v}_F^d - \dot{\mathbf{p}}_F. \tag{25}$$

By substituting (24) into (25) we obtain

$$\tilde{\mathbf{v}}_F = \dot{\mathbf{p}}_{Fd} + b_F\tilde{\mathbf{p}}_F + k_F\overline{\mathbf{p}}_F - \dot{\mathbf{p}}_F \tag{26}$$

and its time derivative becomes

$$\dot{\tilde{\mathbf{v}}}_F = \ddot{\mathbf{p}}_{Fd} + b_F\dot{\tilde{\mathbf{p}}}_F + k_F\tilde{\mathbf{p}}_F - \ddot{\mathbf{p}}_F. \tag{27}$$

Then from (24) and (25) we can rewrite (23) in terms of the linear velocity error as:

$$\dot{\tilde{\mathbf{p}}}_F = \tilde{\mathbf{v}}_F - b_F\tilde{\mathbf{p}}_F - k_F\overline{\mathbf{p}}_F. \tag{28}$$

By substituting (17) and (28) into (27), the time derivative of the linear velocity error can be rewritten as:

$$\dot{\tilde{\mathbf{v}}}_F = \ddot{\mathbf{p}}_{Fd} + b_F\tilde{\mathbf{v}}_F - b_F^2\dot{\tilde{\mathbf{p}}}_F - b_F k_F\overline{\mathbf{p}}_F + k_F\tilde{\mathbf{p}}_F - f(\mathbf{p}_F) - g(\mathbf{p}_F)f_F. \tag{29}$$

The desirable time derivative of the linear velocity error is supposed to be

$$\dot{\tilde{\mathbf{v}}}_F = -c_F\tilde{\mathbf{v}}_F - \tilde{\mathbf{p}}_F. \tag{30}$$

Now, the total thrust f_F, the longitudinal u_{Fx} and the lateral u_{Fy} motion control can be found by subtracting (29) from (30) as follows:

$$\begin{aligned} f_F = (g + \dot{v}_{Lz} + (1 - b_{Fz}^2 + k_{Fz})\tilde{z}_F + (b_{Fz} + c_{Fz})\tilde{v}_{Fz} - b_{Fz}k_{Fz}\overline{z}_F \\ -d(R_{\theta 31}\cos\rho\cos\sigma + R_{\theta 32}\cos\rho\sin\sigma + R_{\theta 33}\sin\rho))\frac{m_F}{c\theta_F c\varphi_F} \end{aligned} \tag{31}$$

$$\begin{aligned} u_{Fx} = (\dot{v}_{Lx} + (1 - b_{Fx}^2 + k_{Fx})\tilde{x}_F + (b_{Fx} + c_{Fx})\tilde{v}_{Fx} - b_{Fx}k_{Fx}\overline{x}_F \\ -d(R_{\theta 11}\cos\rho\cos\sigma + R_{\theta 12}\cos\rho\sin\sigma + R_{\theta 13}\sin\rho))\frac{m_F}{f_F} \end{aligned} \tag{32}$$

$$u_{Fy} = (\dot{v}_{Ly} + \left(1 - b_{Fy}^2 + k_{Fy}\right)\tilde{y}_F + \left(b_{Fy} + c_{Fy}\right)\tilde{v}_{Fy} - b_{Fy}k_{Fy}\bar{y}_F \\ -d(R_{\theta 21}\cos\rho\cos\sigma + R_{\theta 22}\cos\rho\sin\sigma + R_{\theta 23}\sin\rho))\frac{m_F}{f_F}. \tag{33}$$

For the attitude stability, the following nonlinear PD^2 controller (34) proposed in [17] was implemented and tested in simulation for both the leader and the follower:

$$\tau_E = \omega \times J\omega + G(\tilde{\omega}) - (\mu_3 + \mu_2\mu_1)\tilde{\mathbf{q}} - \mu_1 J\dot{\tilde{\mathbf{q}}} - \mu_2\tilde{\omega}. \tag{34}$$

where μ_1, μ_2 and μ_3 are constants.
Next, we show the stability of the follower's translational part.

4.3 Follower controller stability analysis

The following candidate Lyapunov function is chosen for the stability analysis for the follower's translational part with the IBS controller:

$$V = \frac{1}{2}\left(\tilde{\mathbf{p}}_F^T\tilde{\mathbf{p}}_F + \tilde{\mathbf{v}}_F^T\tilde{\mathbf{v}}_F + k_F\bar{\mathbf{p}}_F^T\bar{\mathbf{p}}_F\right) \tag{35}$$

and its time derivative is

$$\dot{V} = \tilde{\mathbf{p}}_F^T\dot{\tilde{\mathbf{p}}}_F + \tilde{\mathbf{v}}_F^T\dot{\tilde{\mathbf{v}}}_F + k_F\bar{\mathbf{p}}_F^T\dot{\bar{\mathbf{p}}}_F. \tag{36}$$

By substituting $\dot{\bar{\mathbf{p}}}_F = \tilde{\mathbf{p}}_F$ and Eqs. (28) and (30) into (36), Eq. (36) becomes

$$\dot{V} = -b_F\tilde{\mathbf{p}}_F^T\tilde{\mathbf{p}}_F - c_F\tilde{\mathbf{v}}_F^T\tilde{\mathbf{v}}_F \leq 0. \tag{37}$$

Finally, (37) is less than zero provided b_F and c_F are positive diagonal matrices, i.e. $\dot{V} < 0, \forall\left(\tilde{\mathbf{p}}_F, \tilde{\mathbf{v}}_F\right) \neq 0$ and $\dot{V}(0) = 0$. It can be concluded from the positive definition of V and applying LaSalle theorem that a global asymptotic stability is guaranteed. This leads us to conclude that $\lim_{t\to\infty}\tilde{\mathbf{p}}_F = 0$ and $\lim_{t\to\infty}\tilde{\mathbf{v}}_F = 0$, which meets the position condition of (6).

4.4 Leader IBS controller

The leader is to track a desired trajectory $\mathbf{p}_{Ld}$. Its IBS controller is developed by following the procedure described for the follower quadrotor.

The result is that the total force and horizontal position control laws f_L, u_{Lx} and u_{Ly} can be written using Euler angles dynamic model representation as:

$$f_L = \left(\ddot{z}_{Ld} + g + \left(1 - b_{Lz}{}^2 + k_{Lz}\right)\tilde{z}_L + \left(b_{Lz} + c_{Lz}\right)\tilde{v}_{Lz} - b_{Lz}k_{Lz}\bar{z}_L\right)\frac{m_L}{c_{\theta L}c_{\varphi L}} \tag{38}$$

$$u_{Lx} = \left(\ddot{x}_{Ld} + \left(1 - b_{Lx}{}^2 + k_{Lx}\right)\tilde{x}_L + \left(b_{Lx} + c_{Lx}\right)\tilde{v}_{Lx} - b_{Lx}k_{Lx}\bar{x}_L\right)\frac{m_L}{f_L} \tag{39}$$

$$u_{Ly} = \left(\ddot{y}_{Ld} + \left(1 - b_{Ly}{}^2 + k_{Ly}\right)\tilde{y}_L + \left(b_{Ly} + c_{Ly}\right)\tilde{v}_{Ly} - b_{Ly}k_{Ly}\bar{y}_L\right)\frac{m_L}{f_L}. \tag{40}$$

The torque vector applied to the leader quadrotor $\tau_{LE} \in \mathbb{R}^3$ is a nonlinear PD^2 controller (34). These leader controllers are used for path tracking tests.

5. Simulations

In order to determine the efficiency of the proposed controller, a MATLAB quadrotor simulator is used to test it numerically. The design parameters of the quadrotor used in the simulator are listed in **Table 1**. Two paths were presented in the simulation to show the performance of using the proposed controller with four different circumstances for quadrotors team formation. The first desired path to be tracked by the leader was.

$$\begin{cases} x_{Ld} = 2\cos(t\pi/80); & y_{Ld} = 2\sin(t\pi/80) \\ z_{Ld} = 1 + 0.1t; & \psi_{Ld} = \pi/6 \end{cases}. \tag{41}$$

The IBS controllers were tested in simulation to track a desired path by the leader and maintain the desired distance, desired incidence angle and desired bearing angle between them for the follower. The parameters chosen for both paths were $b_L = diag(180, 0.34, 0.34)$, $c_L = diag(0.7, 0.02, 0.02)$, $k_L = diag(0.0516, 0.0081, 0.0081)$, $b_F = diag(12, 0.7, 0.7)$, $c_F = diag(1.4, 0.02, 0.02)$ and $k_F = diag(0.01, 0.001, 0.001)$.

The leader initial positions were $\left[x_L, y_L, z_L\right]^T = [2, 0, 0]^T$ metres and the initial angles were $[\varphi_L, \theta_L, \psi_L]^T = [0, 0, 0]^T$ radian. Then the follower followed the leader and maintained the desired distance between them $d = 2$ metres, the desired incidence and bearing angles $\rho = -\pi/6$, $\sigma = \pi/6$ radian, respectively. The follower initial positions were $\left[x_F, y_F, z_F\right]^T = [0.5, 0, 0]^T$ metres and the initial angles were $[\varphi_F, \theta_F, \psi_F]^T = [0, 0, 0]^T$ radian.

The second desired path to be tracked by the leader was

$$\begin{cases} x_{Ld} = 4\cos(t\pi/40); & y_{Ld} = 4\sin(t\pi/40) \\ z_{Ld} = 1 + 0.1t; & \psi_{Ld} = \pi/6 \end{cases}. \tag{42}$$

The leader initial positions were $\left[x_L, y_L, z_L\right]^T = [4, 0, 0]^T$ metres and the initial angles were $[\varphi_L, \theta_L, \psi_L]^T = [0, 0, 0]^T$ radian. Then the follower followed the leader and maintained the desired distance between them $d = 3$ metres, the desired incidence and bearing angles $\rho = 0$, $\sigma = \pi/6$ radian, respectively. The follower initial positions were $\left[x_F, y_F, z_F\right]^T = [1.4, -1.5, 0]^T$ metres and the initial angles were $[\varphi_F, \theta_F, \psi_F]^T = [0, 0, 0]^T$ radian.

The four circumstances included: (17) no disturbance, (32) force disturbance $d_{v_{ix}} = -2$ Nm during $10 \le t \ge 10.25$ seconds, $d_{v_{iz}} = 2$ Nm during

Symbol	Definition	Value	Units
J_x	Roll Inertia	4.4×10^-3	$kg.m^2$
J_y	Pitch Inertia	4.4×10^-3	$kg.m^2$
J_z	Yaw Inertia	8.8×10^-3	$kg.m^2$
m	Mass	0.5	kg
g	Gravity	9.81	m/s^2
l	Arm Length	0.17	m
J_r	Rotor Inertia	4.4×10^-5	$kg.m^2$

Table 1.
Quadrotor parameters.

$20 \leq t \geq 20.25$ seconds, $d_{v_{iy}} = 2$ Nm during $30 \leq t \geq 30.25$ seconds in the first path, $d_{v_{ix}} = -0.5$ Nm during $20 \leq t \geq 20.25$ seconds, $d_{v_{iz}} = 0.5$ Nm during $60 \leq t \geq 60.25$ seconds, $d_{v_{iy}} = 0.5$ Nm during $100 \leq t \geq 100.25$ seconds in the second path, and the attitude part for the leader and the follower is disturbed using (43), applied at the same time for both the leader and the follower, (33) +30% model parameter uncertainty, and (44) −30% model parameter uncertainty.

$$\mathbf{d} = 0.01 + 0.01 \sin(0.024\pi t) + 0.05 \sin(1.32\pi t) \tag{43}$$

Figures 5 and **6** indicate the response of the IBS controller while the leader was tracking the first and second desired path, respectively. **Figure 7** shows the distance

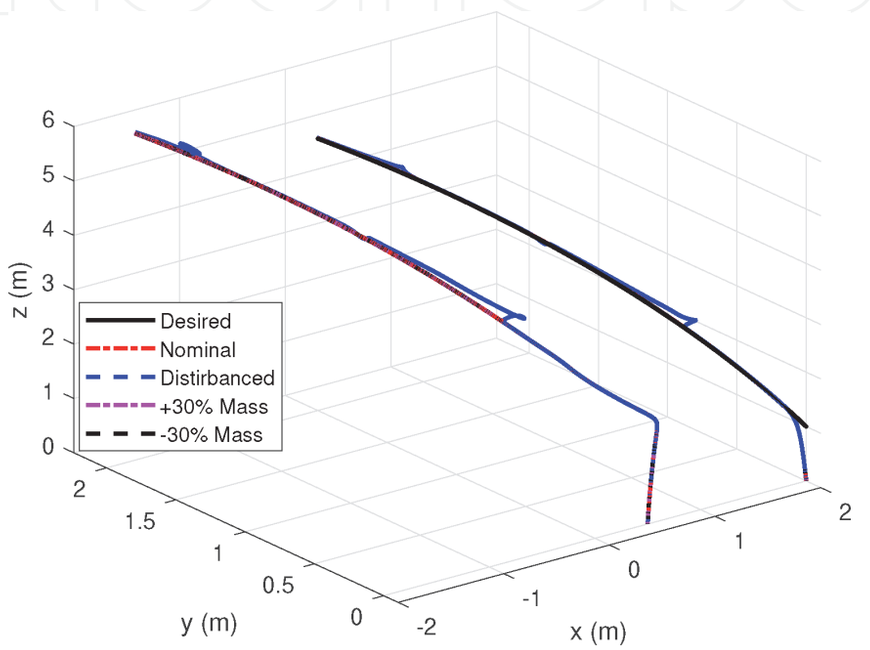

Figure 5.
Leader-follower formation in first path.

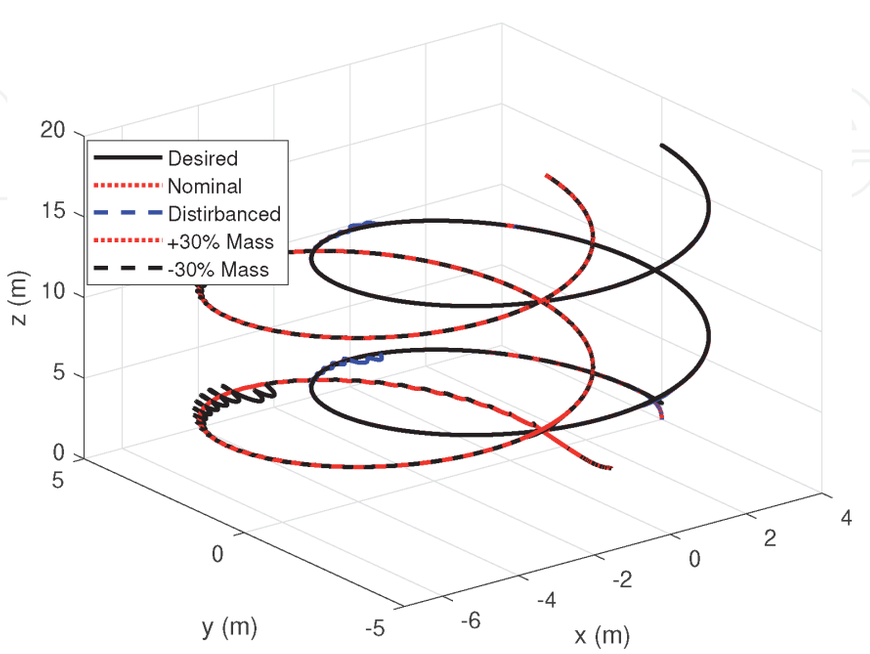

Figure 6.
Leader-follower formation in second path.

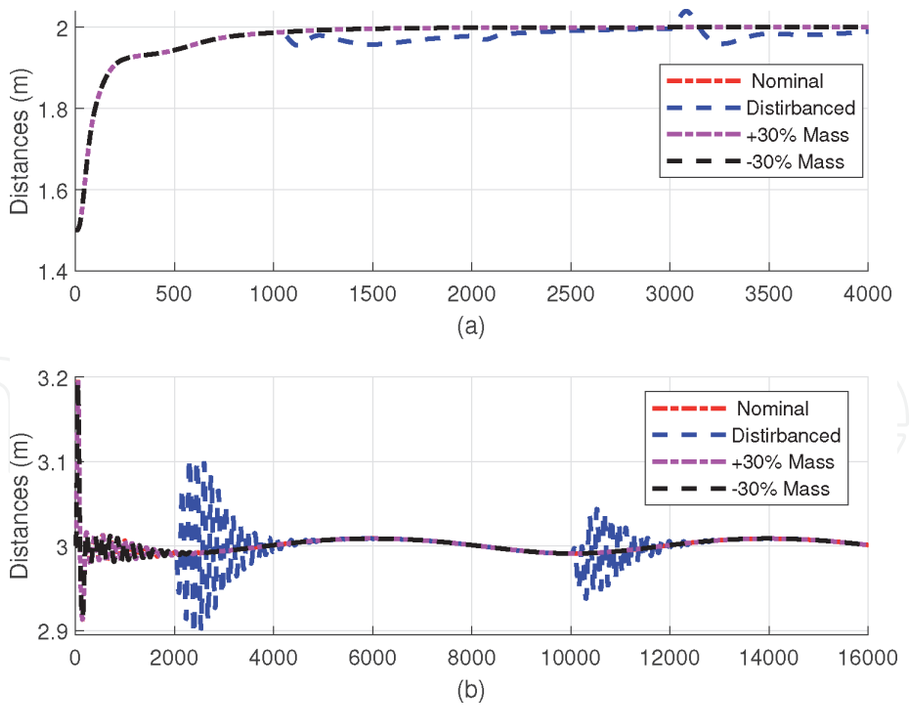

Figure 7.
The distance between the leader and the follower in (a) the first path, (b) the second path.

between the leader and the follower via the two paths, and **Figures 8–11** illustrate the yaw angles' behaviour for the leader and the follower via the two paths respectively.

It can be noticed from these figures that not only the overshoot but also the error in distance between the leader and the follower was low. It was also rejecting the disturbances in the two paths.

Table 2 demonstrates the RMSE values of the two paths positions and yaw angle. It is clear that the RMSE values of the IBS controller were almost the same

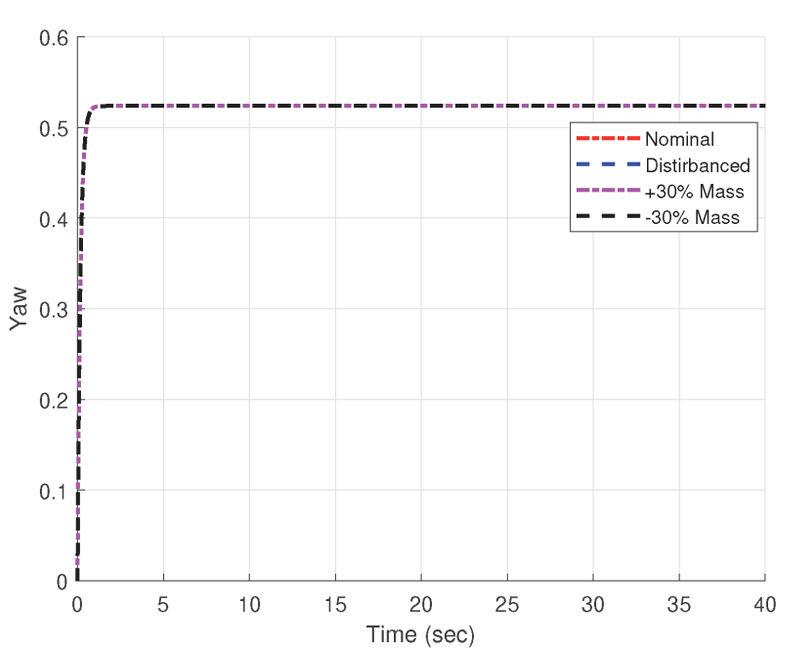

Figure 8.
Leader yaw angle in first path.

when using the IBS controller in normal conditions and with ±30% model parameter uncertainty in both paths, while they significantly increased with the disturbance. It can be seen that the IBS controller was able to track the desired trajectories with small position tracking errors in less than 3 s and it could reject the disturbances and cover the change in model parameter uncertainties.

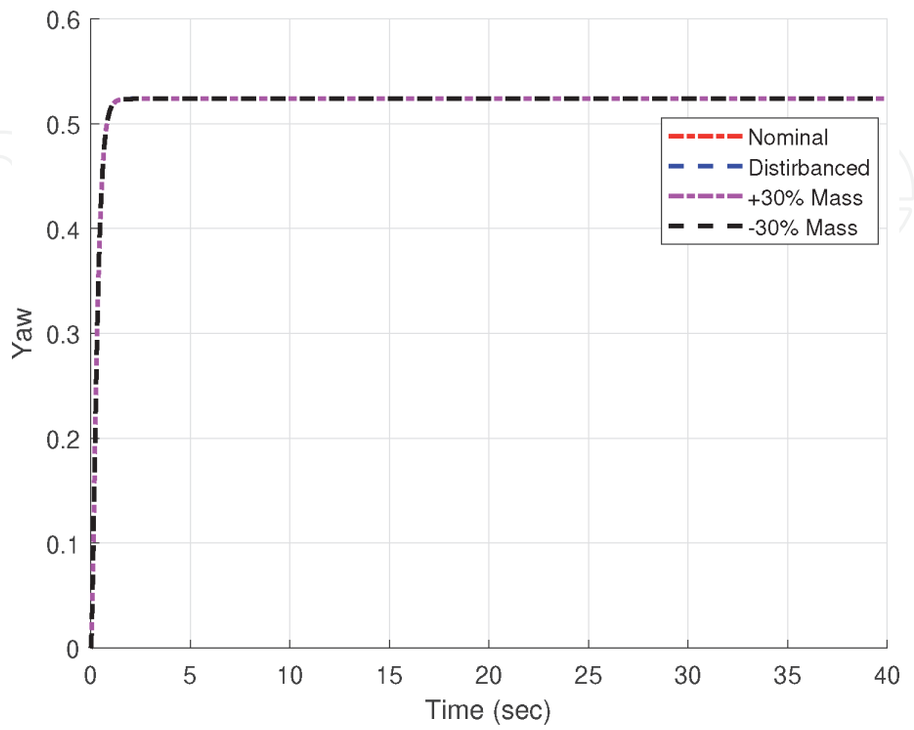

Figure 9.
Follower yaw angle in first path.

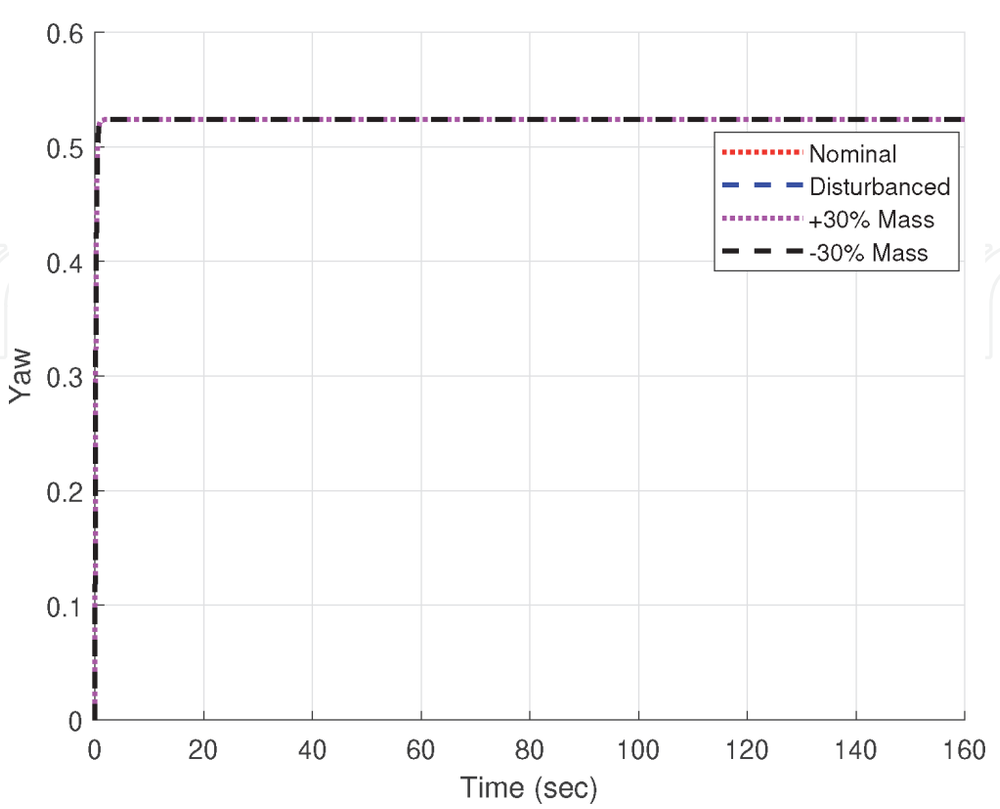

Figure 10.
Leader yaw angle in second path.

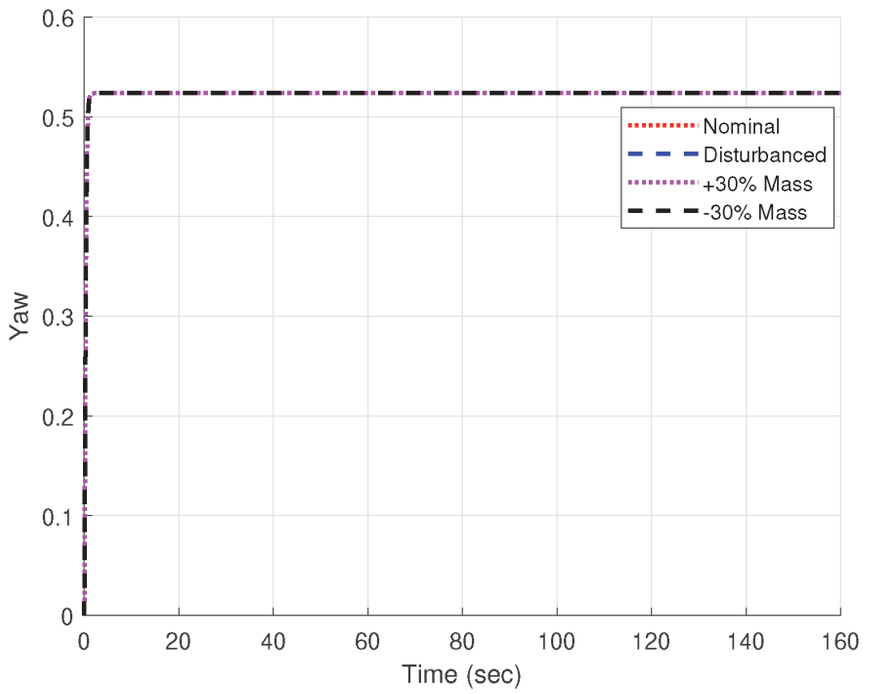

Figure 11.
Follower yaw angle in second path.

	Path 1				Path 2			
RMSE	x (m)	y (m)	z (m)	ψ (deg.)	x	y (m)	z (m)	ψ (deg.)
IBS	0.0005	0.0040	0.0936	0.0004	0.0030	0.0248	0.0936	0
IBS + **d**	0.0112	0.0772	0.0943	0.0004	0.0804	0.1018	0.0910	$7e^{-6}$
IBS + 30%	0.0005	0.0040	0.0936	0.0004	0.0030	0.0248	0.0936	0
IBS − 30%	0.0005	0.0040	0.0936	0.0004	0.0030	0.0248	0.0936	0

Table 2.
Position and ψ RMSE values for the two paths.

In conclusion, it is obvious that the proposed IBS controller maintained the distance between the leader and the follower and keep them in the desired formation.

6. Discussions

This chapter presented an IBS controller derived based on the Backstepping controller for quadrotor UAVs leader-follower team formation problem. Two loops control scheme was used in simulation to find the total thrust and torques. A PD^2 controller was used for attitude part control, while the IBS controller was used to control the translation part of the quadrotors. The dynamic model of the quadrotor was derived based on Euler angles and the effect of the external disturbance and the model parameter uncertainties are also considered.

It is well-known that IBS control is a methodical approach to build the Lyapunov function ahead with the control input design. Thus by the cancellation of the indefinite error terms, the stability of the derivative of the Lyapunov function can

be secured. Although the stability of the Lyapunov function is guaranteed, this does not guarantee the performance of the system. In this work, a suitable Lyapunov function was used to derive the controller stability conditions.

The simulation results prove that the performance by using the IBS controller had significantly small errors. It is also obvious that using the IBS controller led to a smooth and fast performance with small overshoot. Moreover, the response of using the proposed controller in rejecting the external disturbances was fast enough.

As a result, the proposed IBS controller indeed produced good control performance in all circumstances.

Author details

Wesam M. Jasim[1*] and Dongbing Gu[2]

1 College of Computer Science and Information Technology, University of Anbar, Ramadi, Iraq

2 School of Computer Science and Electronic Engineering, University of Essex, Colchester, UK

*Address all correspondence to: co.wesam.jasim@uoanbar.edu.iq

References

[1] Min BC, Cho CH, Choi KM, Kim DH. Development of a micro quad-rotor UAV for monitoring an indoor environment. In: Advances in Robotics. Vol. 5744. Stuttgart, Germany: Holtzbrinck Publishing Group and BC Partners; 2009. pp. 262-271

[2] Srikanth MB, Dydek ZT, Annaswamy AM, Lavretsky E. A robust environment for simulation and testing of adaptive control for mini-UAVs. In: American Control Conference ACC '09. St. Louis, MO, USA: Hyatt Regency Riverfront; 2009. pp. 5398-5403

[3] Erginer B, Altug E. Modeling and PD control of a quadrotor vtol vehicle. In: Proceeding of the 2007 IEEE Intelligent Vehicles Symposium. Istanbul, Turkey; 2007. pp. 894-899

[4] Jaimes A, Kota S, Gomez J. An approach to surveillance an area using swarm of fixed wing and quad-rotor unmanned aerial vehicles UAVs. In: IEEE International Conference on System of Systems Engineering SoSE '08. Singapore; 2008. pp. 1-6

[5] Bouabdallah S, Siegwart R. Full control of a quadrotor. In: Proceeding of the 2007 IEEE/RSJ International Conference on Intelligent Robots and Systems. San Diego, CA, USA; 2007. pp. 153-158

[6] Curiac DI, Volosencu C. Path planning algorithm based on Arnold cat map for surveillance UAVs. Defence Science Journal. 2015;**65**:483-488

[7] Nathan PT, Almurib HAF, Kumar TN. A review of autonomous multi-agent quad-rotor control techniques and applications. In: 2011 4th International Conference on Mechatronics (ICOM). Kuala Lumpur, Malaysia; 2011. pp. 1-7

[8] Pilz U, Popov A, Werner H. Robust controller design for formation flight of quad-rotor helicopters. In: Joint 48th IEEE Conference on Decision and Control and 28th Chinese Control Conference. Shanghai, P.R. China; 2009. pp. 8322-8327

[9] Guerrero JA, Castillo P, Challal Y. Quadrotors formation control a wireless medium access aware approach. Journal of Intelligent and Robotic Systems. 2013;**4**:221-231

[10] Dong X, Yu B, Shi Z, Zhong Y. Time-varying formation control for unmanned aerial vehicles: Theories and applications. IEEE Transactions on Control Systems Technology. 2015;**23**: 340-348

[11] Turpin M, Michael N, Kumar V. Capt: Concurrent assignment and planning of trajectories for multiple robots. The International Journal of Robotics Research. 2014;**33**(1):98-112

[12] Roy N, Newman P, Srinivasa S. Towards a Swarm of Agile Micro Quadrotors. USA, Canada: MIT Press; 2013. p. 504

[13] Nägeli T, Conte C, Domahidi A, Morari M, Hilliges O. Environment-independent formation flight for micro aerial vehicles. In: 2014 IEEE/RSJ International Conference on Intelligent Robots and Systems. 2014. pp. 1141-1146

[14] Saska M, Kasl Z, Preucil L. Motion planing and control of formations of micro aerial vehicles. In: Preprints of the 19th World Congress, the International Federation of Automatic Control IFAC. Cape Town, South Africa; 2014. pp. 1228-1233

[15] Eskandarpour A, Majd VJ. Cooperative formation control of quadrotors with obstacle avoidance and self collisions based on a hierarchical mpc approach. In: 2014 Second RSI/ISM

International Conference on Robotics and Mechatronics (ICRoM). 2014. pp. 351-356

[16] Marquez HJ. Nonlinear Control Systems. New Jersey: Hoboken; 2003

[17] Tayebi A, McGilvray S. Attitude stabilization of a VTOL quadrotor aircraft. IEEE Transactions on Control Systems Technology. 2006;**14**(3): 562-571